Indian Journal of Pure & Applied Physics
Vol. 50, August 2012, pp. 555-565

Model for up-conversion luminescence in silver nanoparticles embedded erbium-doped tellurite glass

S K Ghoshal[1]*, M R Sahar[1], M R Dousti[1], S Sharma[2], M S Rohani[1], R Arifin[1] & K Hamzah[1]

[1]Advanced Optical Material Research Group, Department of Physics, Faculty of Science, Universiti Teknologi Malaysia, 81310 UTM Skudai, Johor, Malaysia

[2]Materials Science Group, Inter-University Accelerator Centre, Aruna Asaf Ali Marg, Vasant Kunj, New Delhi, India

*E-mail: sibkrishna@utm.my

Received 21 Jyly 2011; revised 15 February 2012; accepted 10 May 2012

Nanoparticles (NPs) size dependent enhancement of the infrared-to-visible frequency up-conversion (UC) and absorption coefficient in silver NPs embedded Er^{3+} doped tellurite glasses on pumping with the 976 nm radiation have been investigated. The rate equations derived from the 4-level model developed by the authors earlier to discuss temperature dependent UC have now been extended to study the role played by NPs. The effects of quantum confinement and local field of silver NPs have been incorporated. Considering the spherical NPs size distribution as Gaussian, an analytical expression for the luminescence intensity and absorption coefficient has been obtained for the first time, is further exploited to examine the enhancement of UC emission intensity due to the presence of silver NPs. Furthermore, an enhancement in UC emission intensity of the green bands ($^2H_{11/2}\rightarrow{}^4I_{15/2}$ and $^4S_{3/2}\rightarrow{}^4I_{15/2}$) and red band ($^4F_{9/2}\rightarrow{}^4I_{15/2}$) emission of Er^{3+} ion at temperature 250 K and optimized Er^{3+} concentration 1.0 mol% have been observed up to few times in the presence of silver NPs in the glass. The green emission showed larger enhancement than the red emission. The observed of Er^{3+} luminescence is mainly attributed to the local field effects namely the surface plasmon resonance of silver NPs which causes an intensified electromagnetic field around NPs, resulting in enhanced optical transitions of Er^{3+} ions in the vicinity. The model is quite general and can be applied to other rare earth doped glasses containing metallic NPs. Our results on NPs size dependent emission intensity and absorption coefficient are in conformity with other findings. The present systematic study provides useful information for further development of UC lasers and sensors.

Keywords: Nanoparticles, Up-conversion, Luminescence, Absorption coefficient, Surface plasmon resonance

1 Introduction

The temperature dependent luminescence in erbium-doped tellurite glass without containing metallic nanoparticles, has already been studied[1] (henceforth referred to as I). In the past couple of decades, lanthanide-doped glasses in general and Er^{3+} doped tellurite glasses in particular have attracted special attention due to their potential applications in many optical devices such as UC lasers, sensors, telecommunications, display devices, biological labeling and solar near infrared concentration for photovoltaic exploitation etc.[1-4]. They possesses unusual large infrared transparency, high linear and non-linear refractive indices, good thermal and mechanical stability, excellent corrosion resistance, suitable as a matrix for active element doping, a wide transmission window, lowest cut-off phonon energy, excellent third-order nonlinear optical performance and the highest emission cross-section over the entire range of emission wavelength. The optical and electronic structure properties of these glasses are greatly influenced by the nature of rare earth (RE) dopants, ligand field, multi-phonon relaxation processes, embedded metallic NPs, impurities, temperature and concentration of rare earth ions[5-7]. Meanwhile, erbium doped tellurite glass containing quantum dots or metal NPs stimulated renewed interest in functionalizing the glasses[7,8] by NPs.

Up-conversion luminescence is considered as a promising solution to obtain efficient visible lasers pumped with commercially available infrared laser diodes[1,3,5]. Host materials for rare earth ions play an important role in obtaining highly efficient UC signals[4,7]. Improving the UC efficiency is the key issue in tellurite glasses. Their low maximum phonon energy and high refractive index also yield low non-radiative (NR) decay rates and high radiative emission rates for the energy levels of RE ions[2]. Usually, in order to make devices with optimized photonic properties, the RE ion concentration needs to be kept low to minimize luminescence quenching[8]. However, the absorption cross-section of most of the lanthanide ions is small and needs ways and means to enhance it

for applications. Most the concepts for this enhancement rely on energy transfer from a species with a large absorption cross-section to the rare-earth ion. To achieve enhanced absorption cross-section, use of two or more rare-earth ions together and energy transfer between them and/or use of the metal NPs with rare-earth ions etc. has quite often been found a successful way for this[8-11].

An alternative way to compensate the deleterious effect of quenching is to modify the RE ion environment by embedding metallic nanoparticles[8,12] (NPs). Therefore, glasses containing metallic NPs doped with low concentration of RE ions are of particular interest. The incorporation of metallic NPs in RE doped glasses has been exploited to enhance the UC luminescence efficiency provided the wavelength of the excitation beam or the luminescence is near to the surface-plasmon-resonance wavelength. Recently, optical properties of the rare earth-doped glasses containing NPs have been investigated by many researchers[12-15]. Almeida *et al*[12]. have investigated the Stokes emission in Eu^{3+}-doped TeO_2-PbO-GeO_2 glasses and reported 100% (~2 times) increase in intensity in the hypersensitive transition ($^5D_0 \rightarrow {}^7F_2$) of the Eu^{3+} ion in the presence of gold NPs. The Stokes emission and the effect of silver NPs on the luminescence of Pr^{3+} ions in different glass compositions have been extensively studied by Naranjo *et al*[13]. and Kassab *et al*[14]. Moreover, the influence of metallic NPs on the UC luminescence of rare-earth ions has not much been exploited. Despite of some research work[15-18] that has been carried out in this direction, the mechanism of up-conversion enhancement in the presence of NPs remains debatable yet it still needs considerable theoretical attention. In addition, metal NPs can be introduced easily to concentrations of several atomic per cent into glasses. Much of the studies proposed that the large local field due to metal NPs around the luminescent ion enhances the luminescence efficiency. Interestingly, quantum effects enhance the emission further when the optical frequency of the excitation beam and/or the luminescence frequency of the material are in near resonance with the surface plasmon frequency[19,20] of the NPs.

In order to improve the optical non-linearity to a big extent, various NPs, such as Au, Ag, AgCl, CuCl, CdSe, CdTe, have been reported to be introduced into optical glasses through heat treating, porous glass, ions injecting, ion exchange, sol-gel methods etc.[4,8,21-30]. For instance, enhancement of Eu^{3+} and Er^{3+} luminescence has been reported in fluoroborate glass containing silver NPs couple of years ago[28,29]. Later, experiments were presented where local field or energy transfer effects change the luminescence of RE ion in fluoroborate and silicate glasses[27,30]. Accordingly, luminescence enhancement due to the presence of metallic NPs has been reported for Pr^{3+} and Er^{3+} in oxide glasses but there are not many examples of other glasses being investigated through this approach. The presence of silver NPs enhances the up-conversion fluorescence by about four times, which is ascribed due to local field effect of the silver[29] NPs. Induced optical birefringence in the tellurite glasses containing silver NPs is also reported[31].

Despite of several experimental and few theoretical efforts, the effect of metallic NPs on frequency UC processes and absorption behaviour are far from being understood. Strong UC emission has been observed in silver NPs embedded erbium-doped tellurite glasses at room temperature and the mechanisms of enhanced UC have been analyzed in detail. In the present paper, a simple model investigation have been made to understand the mechanism of the enhanced UC luminescence and absorption coefficient in erbium-doped tellurite glasses as a function of silver NPs sizes. Numerical calculations have been made at temperature 250 K and at optimized Er^{3+} concentration 1.0 mol% on pumping with the 976 nm radiation.

2 The Model

As mentioned in I, a full theoretical calculation of the emission processes and enhanced luminescence in NPs embedded erbium doped tellurite glasses is still lacking due to the formidable difficulties. However, a simplified phenomenological approach is possible. Following I, based on some recent experimental findings we proposed rate equations model to explain two major features of the infrared to visible UC experiments, the enhancement of the UC efficiency for the emission as a function of NPs size and the observed size dependent absorption coefficient. These two items can be explained within an effective four-level model. In addition, an equivalent two level model is quite useful to explain the red and green emission separately. The excitation process consists of two stages, the first being absorption of radiation by bulk glass matrix while the second is the NR excitation of erbium ions by recombining electron-hole pairs. The large values of NR excitation cross-section are due to multi-phonon and impurity

mediated processes under optical pumping in glass matrices. The absorption coefficient of tellurite glasses exceeds by orders of magnitude of the absorption coefficient of erbium. Moreover, the local fields due to the silver NPs caused by quantum confinement effects further enhance the optical response.

The four levels in our model as shwn in Fig. 1, are the ground state $^4I_{15/2}$, and three excited states $^4I_{9/2,}$ $^4F_{9/2}$ and $^4S_{3/2}$ for the red emission; $^2H_{11/2,}$ $^4F_{7/2}$ and $^4F_{9/2}$ and $^4I_{13/2}$, $^4I_{9/2}$ and $^4S_{3/2}$ for the two green emissions, respectively. The corresponding set of rate equations for photons and carriers includes amplified stimulated emission, recombination, NR energy transfer mediated by multi-phonon process and/or a charge transfer through trapping impurities. The

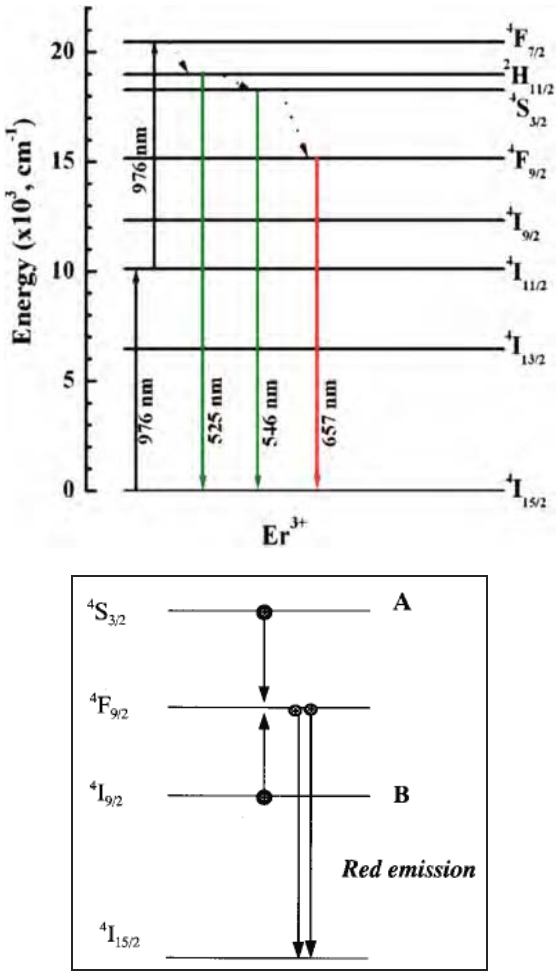

Fig. 1 — (a) Energy levels diagram for a two-step infrared to visible UC of Er^{3+} in tellurite glass under infrared excitation. The upward arrows indicate UC pumping, down arrows indicate radiative transitions and dotted lines show NR decay (upper). (b) Schematic representation of the energy transfer UC processes for the red ($^4F_{9/2}\rightarrow{}^4I_{15/2}$) emission (botom).

ground state is considered as level 1 and other three-excited states as level 2, 3 and 4 along with the increasing direction of energy axis [Fig. 1(a)]. In particular, we assume that the two intermediate levels are empty before the excitation occurs. This allows us to reduce the four level schemes to an effectively two level scheme. The typical four level scheme for a red emission processes is depicted in Fig. 1(b). In the present paper, we complement our treatment in I by investigating the corresponding enhancement of the luminescence due to embedded NPs in the glass. Naturally, therefore, the rate equations derived in I follow as a basic framework of the extended model with NPs.

Once the pumping starts, levels begin to populate and two different NR recombination processes in principle may take place. The first consists in an electron relaxation from energy level 3 to level 2 with the energy given to a second electron which is also present in the same level 3 which is promoted to higher lying levels in the conduction band, from which a very fast relaxation to level 4 occurs. This process involves two electrons in the same level, and therefore, the rate of the process depends quadratically through a coefficient Q_{A1} on the level population N_3. Another NR mechanism involving an electron in the level 3 and a free hole in the valence band edge (level 1) in principle may occur, where the hole is sent deep in the valence band and then very rapidly relaxes again to the band edge. This process has to be proportional, through a coefficient Q_{A2}, to the product of the population of the emitting level 3 (N_3) and the hole concentration in the valence band edge (N_h). The hole concentration N_h equals the total concentration of electrons in the various excited levels, that is $N_h = N_2+N_3+N_4$. Within the four level schemes we proposed, the relaxation times of electrons from levels 4 and level 2 are so fast that N_4 and N_2 are always almost empty, therefore $N_h \approx N_3$. Hence, we end up with a set of four coupled rate equation that has to be integrated. Denote N_i as the level population densities (i=1,.., 4), σ_P the absorption cross-section at the wavelength of the pump, φ_P is the time dependent pumping photon flux and Γ_{ij} are the relaxation rates from the i to the j energy levels. Denoting τ as the total lifetime of the emitting level N_3, B, the stimulated transition rate, which implicitly contains the gain cross-section σ, n_{ph}, is the emitted photons number. The optical mode volume is denoted as V_a, τ_{ph} is the photon lifetime, β is the spontaneous emission factor and τ_r, is the radiative lifetime of N_3

and Q_{nr} is an effective NR decay coefficient equal to $2Q_{A1} + Q_{A2}$. It is possible to observe optical gain whenever the stimulated emission rate is greater than the NR recombination rate. Taking into account both of the two particles recombination processes (e-e or e-h) yield rate equations[1]:

$$\frac{dN_1}{dt} = -\sigma_P \varphi_P(t) N_1 + \Gamma_{21} N_2 \quad \ldots(1)$$

$$\frac{dN_2}{dt} = \frac{N_3}{\tau} - \Gamma_{21} N_2 + Bn_{ph}(N_3 - N_2) + (Q_{A1} + Q_{A2}) N_3^2 \quad \ldots(2)$$

$$\frac{dN_3}{dt} = -\frac{N_3}{\tau} - Bn_{ph}(N_3 - N_2) + \Gamma_{43} N_4 - Q_{nr} N_3^2 \quad \ldots(3)$$

$$\frac{dN_4}{dt} = \sigma_P \varphi_P(t) N_1 - \Gamma_{43} N_4 + Q_{A1} N_3^2 \quad \ldots(4)$$

$$\frac{dn_{ph}}{dt} = -\frac{n_{ph}}{\tau_{ph}} + V_a Bn_{ph}(N_3 - N_2) + \beta \frac{N_3}{\tau_r} \quad \ldots(5)$$

An equivalent NR recombination time can be defined as:

$$\tau_{nr} = \frac{1}{2Q_{nr} N_3} \quad \ldots(6)$$

The rate equation, Eq. (3), in the equivalent two level schemes, that describes excitation of erbium ion, can be written as,

$$\frac{dN_{Er}^*}{dt} = Q_{ex} n_{ex}(N_{Er} - N_{Er}^*) - \frac{N_{Er}^*}{\tau} \quad \ldots(7)$$

where $N_2 = N_{Er}$ is the total concentration of optically active erbium, N_{Er}=N^*_{Er} the concentration of excited erbium, τ the effective lifetime of an erbium ion in the $^4I_{13/2}$ state, n_{ex} the exciton concentration and Q_{ex} is the NR excitation coefficient by a free exciton. The lifetime of excitons (τ_{ex}) is by two orders of magnitude less than the lifetime of erbium ions in the excited state.

Considering the fast subsystem to be in a stationary state one can write the exciton concentration in terms of the absorption coefficient (α) of photons for band-to-band transition as:

$$n_{ex} = \alpha \varphi_P \tau_{ex} \quad \ldots(8)$$

Introducing an effective cross-section of erbium excitation σ_{eff} allows us to write the Eq. (7) in the stationary approximation as:

$$\frac{dN_{Er}^*}{dt} = \sigma_{eff} \varphi_P (N_{Er} - N_{Er}^*) - \frac{N_{Er}^*}{\tau} \quad \ldots(9)$$

with

$$\sigma_{eff} = \alpha Q_{ex} \tau_{ex} \quad \ldots(10)$$

$$\sigma_{eff} = \frac{\alpha}{N_{Er}} \quad \ldots(11)$$

$$\tau_{ex} = \frac{1}{Q_{ex} N_{Er}} \quad \ldots(12)$$

Solving Eq. (9), we arrive at the expression for the time dependent population of excited carriers as:

$$N_{Er}^*(t) = N_{Er} \frac{\sigma_{eff} \varphi_P}{(1 + \sigma_{eff} \varphi_P \tau)} \times \left[1 + \frac{1}{\sigma_{eff} \varphi_P \tau} \exp\left\{ -\frac{t}{\tau}(1 + \sigma_{eff} \varphi_P \tau) \right\} \right] \quad \ldots(13)$$

It is clear from the expression given in Eq. (13) that when, $\sigma_{eff}\varphi_P \to 0$ then $N^*_{Er}(t) \to 0$ as a result $I(t) \to 0$. This expression can be exploited for calculating the pump power dependence of the luminescence intensity. The temperature dependent relationship of emission intensity can be analyzed by considering three level system comprised of $^4I_{15/2}$ (ground state), $^2H_{11/2}$ or $^4S_{3/2}$ or $^4F_{9/2}$ (excited level b) and $^4I_{13/2}$ (excited level a).

3 Formulation of the Emission Intensity

Combining the effects of quantum confinement and the distribution of NPs sizes Φ(L), the luminescence intensity I(L) for the UC, is directly proportional to the total recombination rate (R), population of the excited carriers (N^*_{Er}) and the probability of radiative transition P(L) is written as:

$$I(L) \propto P(L).\Phi(L).N_{Er}^*(t).R \quad \ldots(14)$$

For rare earth doped glass, a relationship exists between the NR decay rate and the total recombination rate. Considering all the possible NR mechanisms, we can write the total decay rate as:

$$\frac{1}{\tau} = R = \frac{1}{\tau_r} + \frac{1}{\tau_{nr}} = R_r + R_{nr} \\ = R_r + (R_p + R_t + R_{Er} + R_{OH} + R_{met}) \quad \ldots(15)$$

In Eq. (15) R_{nr} is the total rate of NR decay, including multi-phonon relaxation rate (R_p), thermal quenching rate (R_t), self-quenching rate (R_{Er}) of Er^{3+}, relaxation rate (R_{OH}) induced by hydroxyl groups and relaxation rate (R_{met}) induced by certain transition metal ions and other rare earth ions[6]. For simplicity, we have ignored last four terms here, as they do not play dominant role as far as the enhancement of UC intensity is concerned. Self-quenching rate (R_{Er}) results from the resonant energy exchange between a pair of Er^{3+} ions. This energy exchange can occur by two mechanisms. One is UC process in which two neighbouring ions pull energy to one, as a result, one comes back to the ground state by NR decay, and the other ion, excited to a higher energy level, returns to the ground state by UC emission. The other is the hopping mechanism, which involves the migration of the excitation energy from one ion to the next. In short, self-quenching rate depends greatly on the concentration of Er^{3+}. The resonant energy transfer model provides the energy transfer rate by dipole–dipole mechanism that can be incorporated in our model[32]. Assuming that the thermal quenching of UC is induced only by the multi-phonon relaxation process, the decay rate can be expressed as the sum of the radiative and multi-phonon relaxation rates R_r and R_p, respectively and is given by, $R = R_r + R_p$. The multi-phonon relaxation rate can be found out by using Bose-Einstein statistics as:

$$R_p(T) = C_p \exp(-\gamma \Delta E)\left[1 - \exp(-\frac{\hbar\omega}{K_B T})\right]^{-p} \quad \ldots(16.1)$$

$$R_p(T) = C_p \exp(-\gamma \Delta E)\left[1 - \exp(-\frac{\hbar\omega}{K_B T})\right]^{-\Delta E/\hbar\omega_{max}} \quad \ldots(16.2)$$

where C_P and γ are NR parameters which depend on the host material, ΔE represents the energy gap between two successive levels (e.g., $^4I_{13/2}$ and $^4I_{15/2}$) and $p = \Delta E/\hbar\omega$ is the number of phonons emitted in the relaxation process. The parameter γ represents a constant related to the electron–phonon coupling constant. In the case of the $^4S_{3/2} - {}^4I_{15/2}$ transition we have chosen $\Delta E = 3000$ cm^{-1}, $C_P = 7.48 \times 10^9$ s^{-1}, $\gamma = 4.7 \times 10^{-3}$ cm, and $\hbar\omega = 750$ cm^{-1}. The best fit with the experimental data is obtained when the multi-phonon relaxation rates are considered as 4-phonon relaxation process of the 750 cm^{-1} frequency vibration. This vibration is associated with the stretching vibrations of TeO_4 and TeO_3 groups.

The radiative decay rate, R_r can be adopted from the experimental law obtained from the variation of the PL intensity versus temperature expressed as:

$$R_r = C_r \exp\left(-\frac{E_r}{K_B T}\right) \quad \ldots(17)$$

where E_r represents the activation energy and C_r is a constant, treated as a fitting parameter. Here, we assumed the weak Arrhenius dependence in describing the rate processes[5].

Now we calculate the optical transition probability, P(L) in the glass host, which is proportional to the probability of finding an electron and a hole in the same local microscopic volume of the glass in the vicinity of the silver NPs. For a spherical NP of diameter L, the volume is $V \sim L^3$ and the surface area is $A \sim L^2$. Since the rate of transition from an excited state to the localized states is proportional to the product of the number of excited photo-carriers and the number of available empty states in steady state condition, the population N_r of photo-carriers in empty states participating in the UC luminescence processes becomes proportional to the product of surface and volume that yields:

$$N_r \propto VA \propto L^5 \quad \ldots(18)$$

The rate of radiative transition depends on the oscillator strength (f) of the exciton, which is inversely proportional to the exciton Bohr radius a_B. However, in case of spherical NPs the transition probability depends on the spatial restriction of carrier motion in the volume due to externally imposed quantum confinement of the NPs. The oscillator strength varies as inverse power law and can be approximated as $f \sim 1/L^\delta$, where power exponent δ depends on the material properties as well as the range of crystallites sizes and shapes being used. For simplicity, we choose $\delta = 3$. Taking the oscillator strength into account, the radiative transition probability in a NP of diameter L becomes:

$$P(L) \propto N_r . f \propto L^2 \quad \ldots(19)$$

Now, the problem boils down to the calculation of the emission intensity with an ensemble of spherical NPs of diameter L having size distribution $\Phi(L)$. The emitted photon energy from the glass will be lower than the optical band gap energy of the material by an amount of the localization energy E_s of the states and the exciton binding energy E_b. Both, in general, are functions of NPs size. The emitted photon energy E_{pl} from the sample can be written as:

$$E_{pl} = h\upsilon = \Delta E_C - E_b - E_s \quad \ldots(20)$$

where ΔE_C is the amount of energy up-shift due to quantum confinement of the silver NPs that cause strong local field in the vicinity of Er^{3+} ion and finally affect the optical band gap of the bulk glass material. The size dependence of optical energy up-shift of NPs according to quantum confinement model yields:

$$\Delta E_C = G / L^{\gamma} \quad \ldots(21)$$

where G and γ are quantum confinement parameters which depend on the geometry and symmetry of NPs.

One can transform Eq. (14) from L to ΔE_C dependence that takes the form

$$I(\Delta E_C) = \int N^*_{Er} R I(L) \Phi(L) \delta(\Delta E_C - G / L^{\gamma}) dL \quad \ldots(22)$$

Taking a normal distribution of silver NPs as Gaussian:

$$\Phi(L) = \frac{1}{s\sqrt{2\pi}} \exp\left[-\frac{(L - L_0)^2}{2s^2} \right] \quad \ldots(23)$$

where L_0 and s are the mean diameter and standard deviation, respectively, for the NPs ensemble. Substituting Eq. (19), Eq. (21) and Eq. (23) into Eq. (22), we obtain the expression for UC emission intensity in terms of N^*_{Er} and R as :

$$I(\Delta E_C) \sim \frac{N^*_{Er} R}{s\sqrt{2\pi}} \left(\frac{G}{\Delta E_C} \right)^{\frac{3+\gamma}{\gamma}} \times \exp\left\{ -\left[\left(\frac{G}{\Delta E_C} \right)^{1/\gamma} - L_0 \right]^2 / 2s^2 \right\} \quad \ldots(24)$$

It is clear from expression given in Eq. (24) that the luminescence intensity depends strongly on the population of excited carriers, total recombination rate, optical energy gap, exciton binding energy and the quantum confinement parameters G and γ arise due to the presence of silver NPs. Therefore, it is important to use the correct quantum confinement model for energy up-shift estimation. The oscillator strength and the exciton binding energy E_b both are complicated functions of the size of NPs and their surrounding media. For simplicity, we took $\gamma = 2$, assuming particle in a box type confinement and G = 4.5 eV at temperature 250 K. The localization energy E_s has taken to be the order of phonon energies, which is about 0.05 eV for optical phonons. Eq. (22) along with Eq. (13) and Eqs (15)-(17) has numerically been solved to generate the luminescence spectra for different diameters of silver NPs and to compare them with experimental findings of Baia *et al*[36].

4 Absorption Coefficient

The optical properties of a silver bulk sample are entirely determined in the visible region by the free electrons, is well known[33,34]. This fact has been established through theoretical and experimental studies on the optical properties of silver particles embedded in glass matrices[33,35]. In most of the experiments, the appearance of a band located at 396 nm associated with the existence of small spherical silver NPs in the electronic absorption spectrum has already been evidenced[33,35]. It has also been argued that, if the particles would not have been spherical (or equi-axial), the absorption band would have appeared at longer wavelengths and gradually shifted to shorter wavelengths as the particles become nearly spherical[33]. Our model calculation relies on the assumption that the NPs within the glass matrix are nearly spherical in shape and subjected to size confinement. In addition, the normalized size distribution of the silver NPs obtained from TEM pictures analysis confirms the Gaussian distribution and the position of the electronic absorption bands found to be located closer to the shorter wavelength which verifies the existence spherical shapes[36,37]. A theoretical approach can also be made in order to determine the dimension of the silver NPs and the model results can be validated.

We used the Mie scattering theory[38] to express the optical absorption coefficient (α) of a collection of uniform silver nanospheres with very small dimensions compared to the wavelength λ of the applied optical field, embedded in a medium of

refractive index n. In the electric dipole approximation and considering that the dielectric constant of the metal is determined by the free electrons, the absorption coefficient can be casted as[33]:

$$\alpha = \frac{9\pi p n^3 c\lambda^2}{\sigma_{dc}\left[(\lambda_m^2 - \lambda^2)^2 + \lambda^2 \frac{\lambda_m^4}{\lambda_a^2}\right]} \quad \ldots(25)$$

where p, σ_{dc}, c and λ_m are the volume fraction of the silver spheres in the glass matrix, the d c electrical conductivity, the velocity of light and the wavelength at which the maximum absorption occurs, respectively. Where the two reduced length scales are:

$$\lambda_a = 2\lambda_c^2 \sigma_{dc} / c \quad \ldots(26.1)$$

and

$$\lambda_c = \frac{(2\pi c)^2 m}{4\pi N_c \varepsilon_m^2} \quad \ldots(26.2)$$

with m, N_c and ε_m representing the electron mass, the number of electrons per unit volume and the complex form of the dielectric constant of the silver particle, respectively. The wavelength for the maximum absorption can be written as:

$$\lambda_m = \lambda_c(\varepsilon_0 + 2n^2)^{1/2} \quad \ldots(27)$$

with ε_0 is the frequency independent part of ε_m, and that the Eq. (25) gives a band of Lorentzian in shape. Following Chakraborty[33], the full width at half maximum (Ω) of this electronic absorption band can be expressed as:

$$\Omega = \frac{\lambda_m^2}{\lambda_a} = \frac{(\varepsilon_0 + 2n^2)c}{2\sigma_{dc}} \quad \ldots(28)$$

The *dc* conductivity σ_{dc} is given by:

$$\sigma_{dc} = \frac{N_c e^2 L}{2mu_F} \quad \ldots(29)$$

where e is the electron charge, L is the *NP* diameter and the electron velocity at the Fermi energy is given by:

$$u_F = \left(\frac{2E_F}{m}\right)^{1/2} \quad \ldots(30)$$

By substituting the expression of σ_{dc} in Eq. (28) one obtains:

$$\Omega = \frac{(\varepsilon_0 + 2n^2)cmu_F}{N_c e^2 L} \quad \ldots(31)$$

In Eq. (31), substituting the half-width value of the experimental absorption band (~ 5-50 nm) recorded from the glass sample at various concentration of silver compound, $N_c e^2/m$ ~ 1.72×10^{31}, ε_0 = 4.9, u_F ~ 1.43×10^6 ms^{-1} and by considering the refractive index n = 1.5 for the glass matrix a *NP* diameter ~ 4-50 nm are obtained. The electronic absorbance A_e in terms of the concentration of the species C_o and the thickness h of the sample can be expressed as a function of the absorption coefficient α as follows:

$$A_e = \alpha C_0 h \quad \ldots(32)$$

Using the measured values of absorbance for the sample with the silver oxide concentration from 0.05-0.3 mol% and its thickness (0.2 – 1.5 mm) the experimental absorption coefficient as a function of wavelength can be obtained. The unknown value of the volume fraction of the silver spheres p in Eq. (25) has been obtained by adjusting the experimental absorption coefficient amplitude to the theoretical one. The value of λ_m has been obtained using the data from the experimental findings[8,38].

The relation between the intensity of up-converted fluorescence I(ΔE_C), the excitation power (P_{exc}) and the number of photons (n_{ph}) involved in UC process yields,

$$I(\Delta E_C) \propto (P_{exc})^{n_{ph}} \quad \ldots(33)$$

Singh *et al*. found the experimental slopes of the two green bands (525 nm and 546 nm) and the red band (657 nm) that fits well with n_{ph} ~ 2 indicating that two incident near-infrared photons are involved for each emitted visible photon[8]. However, our model fits well with n_{ph} ~ 4, indicating that four photons processes are involved for the UC emission. This overestimation may be due to the simplicity of the model and that requires further attention. Following Singh *et al*[8]., the mechanism involved in the UC emission processes are shown schematically in the energy level diagram of the Er^{3+} ion in Fig. 1. The first incident photon is absorbed by the Er^{3+} ion and promoted to $^4I_{11/2}$ ($^4I_{15/2}\rightarrow{}^4I_{11/2}$) level. The absorption of second incident photon promotes the Er^{3+} ion to

higher lying $^4F_{7/2}$ ($^4I_{11/2} \rightarrow {}^4F_{7/2}$) state. The excited ions in the $^4F_{7/2}$ state decay non-radiatively to the lower excited states $^2H_{11/2}$ and $^4S_{3/2}$. The Er^{3+} ions in these states decay radiatively to ground state via $^2H_{11/2} \rightarrow {}^4I_{15/2}$ and $^4S_{3/2} \rightarrow {}^4I_{15/2}$ transitions and non-radiatively to $^4F_{9/2}$ state followed by radiative decay via $^4F_{9/2} \rightarrow {}^4I_{15/2}$ transition.

5 Results and Discussion

Solving the rate equations of four levels model,one gets the emitted photon numbers. Using Eqs (13), (16), (17) and (24), the pump power dependence of luminescence intensity has been calculated as shown in Fig. 2 to demonstrate a strong correlation between erbium and exciton photoluminescence in the presence of NPs. These equations has been solved by taking NR lifetime of 20 ns, gain cross-section of 1.2×10^{-17} cm^2, density of Er^{3+}~ 6×10^{19} cm^{-3}, pumping photon flux of 10^{18} photons/(s cm^2), τ = 3.86 ms, stimulated emission cross-sections ~ 9.0×10^{-21} cm^2, phonon energy[7,9,32] of the host glass as 760 cm^{-1} and 1.0 mol% Er^{3+} at 250 K. We have taken, R_r = 3528 s^{-1}, $C_r = 1.3 \times 10^5$ s^{-1} and E_r ~ 59 meV. It is found that the efficiency for the red emission is higher than the green emission. This is due to more NR processes are involved in the green UC than the red one.

Figure 2 shows that at low pumping intensity the lifetime of exciton is determined mainly by the NR process assisted by Er^{3+} excitation. It should be noted also that with an increasing pump power, i.e. the amount of excited erbium, effective cross-section would increase. This result is determined by the fact that the band-to-band absorption coefficient is an intrinsic property of the host matrix, and does not depend on the concentration of erbium dopant (as is the case for excitation of erbium in dielectric matrices). Under these conditions the probability to excite a single ion increases when the total number of excitable ions decreases at a given photon flux. The reason for the lower value of the effective cross-section as compared to the pure radiative case may possibly arise due to NR processes that control the lifetime. The presence of silver NPs enhances the UC emission intensity further as compared to samples without NPs.

The results for the NPs size dependent peak intensity are shown in Fig. 3. The intensity of the green bands is found to increase rapidly as compared to the red bands with increasing size of NPs. This particular observation can be explained in terms of the charge cloud effect of the plasmon band associated with the metal NPs. It is worth mentioning that the charge cloud of the plasmon band affects more to the levels occur nearer to the plasmon frequency band of silver i.e. the levels giving green bands and hence they show larger increase as compared to the far lying red bands. As the size of NPs is increased the emission intensity of these bands is also increased as the larger particles believed to have strong plasmon oscillations. Furthermore, silver NPs can enhance the intensity of Er^{+3} bands following two different mechanisms, firstly, by energy transfer from silver plasmon band to Er^{+3} ion, and secondly, through local field of silver NPs on Er^{3+} ions. A direct excitation of the plasmon band seems less probable because the excitation wavelength (976 nm) of the pumping radiation is far away from the surface plasmon band of silver NPs.

The enhancement in the intensity is probably due to local field of silver NPs. Malta *et al*[39]. have reported that in the presence of small sized NPs in the glass matrix, the possibility of energy transfer from metal

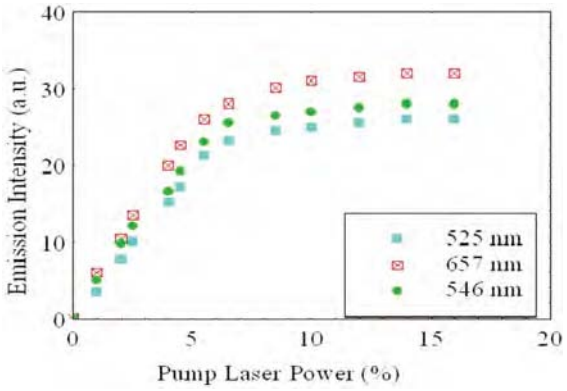

Fig. 2 — Pump power excitation dependent intensity of the up-converted red and green emission from Er^{3+} for 1.0 mol% Er^{3+} and silver oxide concentration 0.05-0.3 mol% at T = 250 K

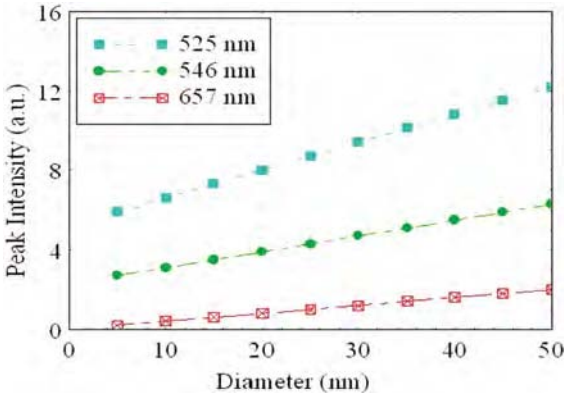

Fig. 3 — Silver NPs size dependent fluorescence peak intensity of the up-converted red and green emission from Er^{3+} for a 1.0 mol% Er^{3+} and silver oxide concentration 0.05-0.3 mol% at T = 250 K

NPs to rare earth becomes insignificant which was subsequently verified by the lifetime analysis. Singh *et al*[8]. recorded the decay pattern of the Er^{3+} for $^4S_{3/2} \rightarrow {}^4I_{15/2}$ transition and carefully analyzed the decay pattern. Two important facts were noticeable in this study. Firstly, the decay curve for both the samples doped with silver NPs and un-doped samples were almost overlapped on each other, and secondly, there was no rise time in any case. These two observations clearly ruled out the possibility of energy transfer from the plasmon level to erbium ion. Therefore, the local field effect due to NPs is believed to play a crucial role in enhancing the fluorescence intensity corresponding to different bands.

The results for the NP size dependent absorption coefficient are shown in Fig. 4. By inspecting the curves, one can see a gradual increase of the half-width of the electronic absorption band as the silver content becomes higher or size of NPs are decreased. The dependence of bandwidth upon particle size, i.e. $\Omega \sim 1/L$, results from the changing mean free path of the electrons[33] and shows the increase of the bandwidth with the decrease of the cluster size. It is important to mention that our model can be applied only if the mean free path of the electrons is equal to the particle size. The agreement of our bandwidth values with the experimental UV–VIS spectra of the silver-doped glasses confirms the validity of the above explanation. In actual experimental situation the presence of very small NPs with diameter of only a few of nanometers is quite feasible and is responsible for the enlargement of the absorption bandwidths (Fig. 4).

Assuming that the maximum value of the absorption bands is preserved, we used a different scenario to explain their broadening. It is believed that the presence of silver particles with the same size but with different, spherical ($< \lambda_m$) and non-spherical ($> \lambda_m$) shapes, may be responsible for the broadening. We consider that this kind of broad electronic absorption band as a convolution of these bands. The TEM picture of the sample principally confirms the first hypothesis; a wide particles distribution of almost spherical shapes with diameter in the range 4-10 nm has also been observed[36]. Although, it is difficult to examine in detail the shapes of such small particles at nanoscale, however, the second hypothesis of multiple shape and size distribution cannot be excluded. As mentioned earlier, for higher silver content the existence of almost spherical silver particles with different diameter, mainly below 4.0 nm, has been evidenced from TEM measurements. Therefore, our assumption on Gaussian distribution of spherical NPs is justified. A realistic model must emphasize the presence of silver NPs with almost spherical shapes and a large variety of dimensions within the glass matrix for such small doping contents. In order to determine more precisely the shapes and symmetry of particles further UV–VIS experiments with polarized light are needed[40]. It is important to note that NPs with diameter below 2 nm are better treated as molecular clusters and their plasmon band is strongly damped and could even disappear.

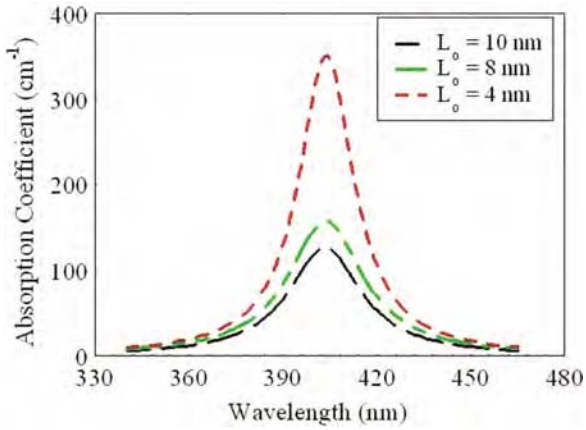

Fig. 4 — Silver NPs size dependent absorption coefficient for a 1.0 mol% Er^{3+} and silver oxide concentration 0.05-0.3 mol% at T = 250 K

6 Conclusions and Further Outlook

In the present paper, the NP size dependent enhancement of infrared-to-visible frequency UC and absorption coefficient in erbium-doped tellurite glasses excited by laser radiation at 976 nm by developing a model, have been studied. The rate equations are derived using both 4-level and equivalent 2-level schemes and the results on pump power dependent emission intensity, size dependent absorption coefficient and UC intensity are presented at temperature 250 K at fixed concentration 1.0 mol% of erbium. The presence of silver NPs enhances the UC fluorescence of the green bands ($^2H_{11/2} \rightarrow {}^4I_{15/2}$ and $^4S_{3/2} \rightarrow {}^4I_{15/2}$) and red band ($^4F_{9/2} \rightarrow {}^4I_{15/2}$) emission of Er^{3+} ion by about few times, which is ascribed due to local field effect of the silver NPs. It is observed that size dependent enhancement of the green emission is large as compared with those of the red transition. The enhancement has been analyzed in terms of the local field effect due to the silver NPs. The absorption

coefficient is found to be highly sensitive to the size of NPs. By controlling a set of fitting parameters in the model, it is possible to tune the size dependent luminescence peak, full width at half maxima, the emission intensity and the absorption coefficient. The results suggested that both quantum confinement and local field effects determine the optical and electronic properties of these glasses.

Through our phenomenological model, we have established that incorporation of silver NPs leads to a drastic change in the absorption coefficient within the wavelength range 340-460 nm. Our study indicates the principal role-played by the silver NPs, in particular their surface plasmon resonance contribution to the observed absorption coefficient. However, a Judd–Ofelt analysis of these glasses are needed that might have some applied interest for optically stimulated quantum electronic devices, optically operated fibers and may also be promising for application in self-frequency conversion. The present study could create new perspectives for the development of advanced glass materials and understanding their optical properties, thanks to the large variety of silver NPs dimensions existent within the tellurite glass matrix for even substantially small doping contents. Our theoretical model and the numerical analysis are qualitatively well consistent with experimental data. It is hoped that our rate equations may provide useful information for exploiting NPs embedded RE doped tellurite glasses in fabricating UC lasers and sensors. In addition, this model can be extended to examine the excited state dynamics, the temporal behaviour of UC emission and NPs size dependent Stokes emission for red and green transitions. A complete microscopic model, however, requires the incorporation of the local bonding environment, the local vibrational density of states of the rare earth ion within the matrix, detail nature on shape and size of NPs and effect of surface plasmon polariton because some of these modes may or may not be coupled to electronic excited states.

Acknowledgement

The financial support from RMC, UTM through the research grant (VOTE 4D005 and Q.J130000.7126.00J39/GUP) are gratefully acknowledged.

References

1 Ghoshal S K, Sahar M R, Rohani M S & Sharma S, *Indian J Pure & Appl Phys,* 49 (2011) 509.
2 Xu S, Fang D, Zhang Z & Jiang Z, *J Solid State Chem,* 178 (2005) 1817.
3 Xiao K & Yang Z, *Opt Mater,* 29 (2007) 1475.
4 Rai V K & Rai S B, *Appl Phys B,* 87 (2007) 323.
5 Pan Z, Udea A, Mu R & Morgan S H, *J Lumin*, 126 (2007) 251.
6 Dai S, Yu C, Zhou G, Zhang J, Wang G & Hu L, *J Lumin,* 117 (2006) 39.
7 Giri N K, Singh A K & Rai S B, *J Appl Phys,* 101 (2007) 033102.
8 Singh S K, Giri N K, Rai D K & Rai S B, *Solid State Sc,* 12 (2010) 1480.
9 Jlassi I, Elhouichet H, Ferid M & Barthou C, *Opt Mater*, 32 (2010) 743.
10 Tikhomirov V K, Drisen K, Walrand C G & Mortier M, *Opt Exp,* 15 (2007) 9535.
11 Feifei C, Tiefeng X, Shixun D, Qiuhua N, Xiang S, Jianliang Z & Xunsi W, *Opt Mater*, 32 (2010) 868.
12 Almeida R de, Silva D M da, Kassab L R P & Araújo Cid B de, *Opt Comm,* 281 (2008) 108.
13 Naranjo L P, Araújo Cid B de, Malta O L, Cruz P A S & Kassab L R P, *Appl Phys Lett*, 87 (2005) 241914.
14 Kassab L R P, Araújo Cid B de, Kobayashi R A, Almeida Pinto R de & Silva D M da, *J Appl Phys,* 102 (2007) 103515.
15 Ueda J, Tanabe S & Ishida A, *J Non-Cryst Sol,* 355 (2009) 1912.
16 Silva D M da, Lüthi S R, Araújo Cid B de, Gomes A S L & Bell M J V, *Appl Phys Lett,* 90 (2007) 081913.
17 Rai V K, Menezes L de S, Araújo Cid B de, Kassab L R P, Silva D M da & Kobayashi R A, *J Appl Phys,* 103 (2008) 093526.
18 Zhang F, Braun G B, Shi Y, Zhang Y, Sun X, Reich N O, Zhao D & Stucky G, *J Am Chem Soc,* 132 (2010) 2850.
19 Flytzanis C, Hache F, Klein M C, Ricard D & Roussignol Ph, *Progress in Optics XXIX, Elsevier Science* (E. Wolf Ed., Amsterdam), 1991.
20 Hayakawa T, Selvan S & Nogami M, *Appl Phys Lett,* 74 (1999) 1513.
21 Zhao Zhenyu, Jia Tianqing, Lin Jian, Wang Zugeng & Sun Zhenrong, *J Phys D: Appl Phys,* 42 (2009) 045107.
22 Madden S J & Vu K T, *Opt Exp,* 17 (20) (2009) 17645.
23 Lin H, Meredith G, Jiang S, Peng X, Luo T, Peyghambarian N & Pun E Y B, *J Appl Phys*, 93(1) (2003) 186.
24 Lin J, Huang W H, Sun Z R, Ray C S & Day D E, *J Non-Cryst Sol,* 336(3) (2005) 189.
25 Mirgorodsky A P, Soulis M, Thomas P, Merle-Mjean T & Smirnov M, *Phys Rev B*, 73 (2006) 134206.
26 Lin Jian, Huang Wenhai, Li Bofang, Jin Chong, Liu Changcheng, Lei Shuhua & Sun Zhenrong, *J Mat Sc Tech,* 24 (2008) 863.
27 Eroni F, Santos P dos, Fávero F C, Gomes A S L, Xing J, Chen Q, Fokine M & Carvalho I C S, *J Appl Phys,* 105 (2009) 024512.
28 Carmo A P, Bell M J V, Anjos V, Almeida Ricardo de, Silva Davinson M da & Kassab L R P, *J Phys D: Appl Phys,* 42 (2009) 155404.
29 Kassab L R P, Almeida Ricardo de, Silva Davinson M da, Assumpção Thiago A A de & Araújo Cid B de, *J Appl Phys,* 105 (2009) 103505.
30 Kassab L R P, Almeida Ricardo de, Silva Davinson M da & Araújo Cid B de, *J Appl Phys,* 104 (2008) 093531.
31 Murai Shunsuke, Hattori Ryosuke, Fujita Koji & Tanaka Katsuhisa, *Appl Phys Exp,* 2 (2009) 102001.

32 Auzel F, Bonfigli F, Gagliari S & Baldacchini G, *J Lumin*, 94 (2001) 293.
33 Chakraborty P, *J Mat Sc*, 33 (1998) 2235.
34 Doremus R H, *J Chem Phys,* 42 (1965) 414.
35 Otter W, *Z Phys*, 161 (1961) 163.
36 Baia L, Muresan D, Baia M, Popp J & Simon S, *Vibr Spect,* 43 (2007) 313.
37 Pan Z, Ueda A, Aga Jr R, Burger A, Mu R & Morgan S H, *J Non-Cryst Sol,* 356 (2010) 1097.
38 Mie G, *Ann Phys,* 225 (1908) 377.
39 Malta O L & Santos M A C dos, *Chem Phys Lett,* 174 (1990) 13.
40 Kassab L P R, Freitas L Ferreira, Ozga K, Brik M G & Wojciechowski A, *Opt Laser Tech,* 42 (2010) 1340.